Archive of Applied Mechanics manuscript No.
(will be inserted by the editor)

Kijun Park

Exclusive Single Pion off the Proton: Results from CLAS

Received: February 17, 2016/ Accepted: date

Abstract Exclusive meson electroproduction off protons is a powerful tool to probe the effective degrees of freedom in excited nucleon states at the varying distance scale where the transition from the contributions of both quark core and meson-baryon cloud to the quark core dominance. During the past decade, the CLAS collaboration has executed a broad experimental program to study the excited states of the proton using polarized electron beam and both polarized and unpolarized proton targets. The measurements covered a broad kinematic range in the invariant mass W and photon virtuality Q^2 with nearly full coverage in polar and azimuthal angles in the hadronic CM system. As results, several low-lying nucleon resonance states in particular from pion threshold to $W < 1.6$ GeV have been explored. These include $\Delta(1232)\frac{3}{2}^+$, $N(1440)\frac{1}{2}^+$, $N(1520)\frac{3}{2}^-$, and $N(1535)\frac{1}{2}^-$ states. In addition, we recently published the differential cross-sections and helicity amplitudes of the reaction $\gamma^* p \to n\pi^+$ at higher W (1.6 to 2.0 GeV) which are the $N(1675)\frac{5}{2}^-$, $N(1680)\frac{5}{2}^+$, and $N(1710)\frac{1}{2}^+$ states. These excited states with isospin 1/2 and with masses near 1.7 GeV can be accessed in single $n\pi^+$ production as there are no isospin 3/2 states present in this mass range with the same spin-parity assignments.

I will briefly discuss these states from CLAS results of the single charged pion electroproduction data.

Keywords CLAS · single pion electroproduction · helicity amplitude, $N(1440)\frac{1}{2}^+$, $N(1520)\frac{3}{2}^-$, $N(1535)\frac{1}{2}^-$ · $N(1675)\frac{5}{2}^-$, $N(1680)\frac{5}{2}^+$, $N(1710)\frac{1}{2}^+$ · more

1 Introduction

The structure of the nucleon and its excited states has been one of the most extensively investigated subjects in nuclear and particle physics for several decades, because it allows us to understand important aspects of the underlying theory of the strong interactions. Many different reactions can be used to study the properties of the nucleon and its excited states. The inclusive electron scattering spectrum clearly indicates four resonance regions above the elastic peak. However, it does not allow us to separate excited states with different isospin and J^P quantum numbers which make up the second and higher resonance peaks. Even in the first resonant region there is a considerable non-resonant background under the dominant $\Delta(1232)$ peak. Therefore, exclusive measurements with a full angular coverage in the hadronic center-of-mass (CM) are necessary to separate the non-resonant contributions from the resonance contributions. A fit of the angular distributions and the W dependence within reaction theories or models allows to determine relative strengths for different resonances. In particular,

Jefferson Lab
12000 Jefferson Ave, Newport News, VA 23606 USA
Tel.: +1-757-269-6989
E-mail: parkkj@jlab.org

rapidly decaying into meson nucleon final states are interested in because of the small mass of the pion, the single pion-nucleon decay is the favorite channel for many lower mass resonances. Moreover, a single pion electro-production is being extensively exploited to understand the structure of nucleon. In order to establish a better understanding of the connection between the dressed quark regime and the perturbative QCD domain at high Q^2, it is important to measure fundamental observable, such as cross-sections and asymmetries in the resonance region.

On the fundamental level there exists only a very limited understanding of the relationship between Quantum Chromo-Dynamics (QCD), the field theory of the strong interaction, and the constituent quark models (CQM) or alternative hadron models, although recent developments in Lattice QCD, most notably the predictions of the excited strangeness $S = 0$ baryon spectrum of N^* and Δ^* states, have shown [1] that the same symmetry of $SU(6) \otimes O(3)$ is likely at work here as is underlying the spectrum in the CQM. The various current resonance models predict not only different excitation spectra but also different Q^2 dependence of transition form factors [2]. The mapping of the transition form factors of resonances with full range of invariant W region will help us to better understand the underlying quark or hadronic structures [3]. Experimentally, a sufficient and complete data will help to uncover unambiguously the structure of the nucleon and its excited states in the entire resonance mass range.

Recently, precise data [4; 5; 6; 7; 8; 9; 10; 11] allow to determination of $\Delta(1232)\frac{3}{2}^+$ for the magnetic dipole transition form factor and the electric and scalar quadrupole transition, covering a range of $0 \le Q^2 \le 7$ GeV^2. One of the major results of these analyses is the clear evidence for the presence of significant meson-baryon contributions to the resonance formation, which at low Q^2 are of the same magnitude as the quark contribution, but fall off more rapidly with increasing photon virtuality Q^2. A reasonable description of the $\gamma^* p \to \Delta(1232)\frac{3}{2}^+$ transition was achieved in the models that include pion-cloud contribution [12; 13] and also in the dynamical reaction models, where the missing strength has been attributed to dynamical meson-baryon interaction in the final state [14; 15; 16; 17; 18].

From much more data [19; 20; 21] for beyond $\Delta(1232)\frac{3}{2}^+$, similar conclusions have been drawn for the excited nucleon states $N(1440)\frac{1}{2}^+$, $N(1520)\frac{3}{2}^-$ and $N(1535)\frac{1}{2}^-$ [22; 23; 24] using a relativistic quark model with spectator di-quark. The results of this effort has been extensively discussed in recent reviews [2; 25]. Moreover, the higher mass range $W > 1.6$ GeV shows many N^* and Δ^* resonances are populated [26]. Several of them have significant branching ratio into the $N\pi$ final state and can be investigated with exclusive single pion channel, while others couple more strongly to $N\pi\pi$ final states. Of course, a full exploration should be done by requiring several final states to be measured and analyzed together in a coupled channel framework. Providing essential input to full coupled-channel analyses allows us to expect for some resonances, especially $N(1675)\frac{5}{2}^-$, and $N(1680)\frac{5}{2}^+$ that a single channel analysis will yield reliable results due to the large coupling of these states to $N\pi$ and the absence of $I = \frac{3}{2}$ states with the same spin-parity in that mass range.

In this proceeding I summarize some of the highlighted results from analysis of differential cross sections for the process $ep \to e'\pi^+ n$ in the range of W from near pion production threshold to deep inelastic scattering regime (up to 2.4 GeV) with nearly full azimuthal and polar angle coverage in the $\pi^+ n$ system.

2 Summary

The CLAS detector covers a very large kinematic range in the four CM variables W, Q^2, $\cos\theta^*_\pi$, ϕ_π. For further analysis the data binning was matched to the underlying physics to be extracted. The study of nucleon excitation requires the analysis of the azimuthal ϕ^*_π dependence of the differential cross section to determine the separated structure functions and the analysis of the polar angle dependence to identify the partial wave contributions at a given invariant mass of the hadronic final state. The binning in the hadronic mass W must accommodate variations in the cross section, taking into account the width of resonances and their threshold behavior. On the other hand the Q^2-dependence is expected to be smooth. We have collected large number of kinematic bins, the resulting over 33,000 differential cross-sections, 4,000 asymmetries for $1.11 < W < 1.67$ GeV and 37,000 differential cross sections for $1.6 < W < 2.0$ GeV region and 140 differential cross-sections for DIS regime through several dedicated analyses.

The extraction of axial form factor (G_A) and generalized form factor with dipole form factor (G_1/G_D) in near threshold $W = 1.11$ GeV is done by multipole analysis [27], which is shown in Fig. 1. The data shows a good agreement with Light Cone Sum Rule (LCSR) that provides most directly relation of the hadron form factors and nucleon distribution amplitude (DA) that enter info pQCD calculation without double counting.

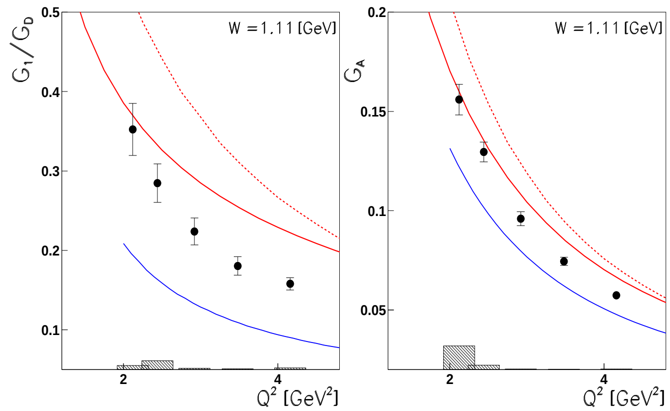

Fig. 1 (color online) Q^2 dependence for $n\pi^+$ of G_1 normalized by the dipole form factor (left) and axial form factor G_A (right). Shaded bars show the systematic errors. Various models are presented, blue solid line: MAID2007 for E_{0+}/G_D, and red solid-dash lines: LCSR (red solid is the LCSR calculation using experimental electromagnetic form factors as input an d red dash is pure LCSR) [28].

A series of analyses of use not only the exclusive single pion electroproduction but other meson production channels (π^0, η, 2π) allowed to extract several nucleon excitation states. These N^* results are obtained from data analyses within Unitary Isobar Model (UIM) and Dispersion Relations (DR). These data sets cover Q^2 range from 1.8 to 4.0 GeV^2. The employed approaches of UIM and DR were described in detail in Refs. [29; 33] and have been used successfully in Refs. [33; 32; 31] for the analyses of pion-electroproduction data in a wide range of Q^2 from 0.16 to 6 GeV^2.

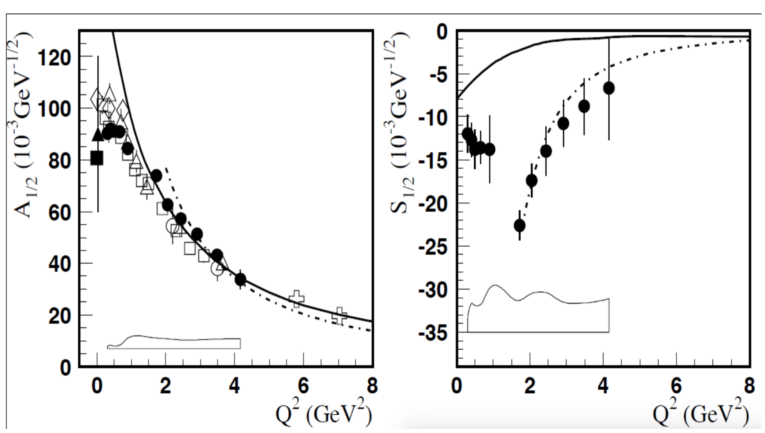

Fig. 2 Transition Form Factors for $N(1535)1/2^-$ with $\beta_{N\pi} = 0.485$, $\beta_{N\eta} = 0.460$. The solid boxes are the results extracted from η photo- and electroproduction data in Ref. [30], the open boxes show the results from η electroproduction data [34; 35; 36]. Sensitive to long. as well (strong interference S_{11}-P_{11}), solid: LFRQM, dash-dot: LCSR

Figure 2 shows helicity amplitudes ($A_{1/2}$, $S_{1/2}$) for $N(1535)1/2^-$ as one of the second resonance region from the analysis results. The $A_{1/2}$ confirms the Q^2-dependence of this amplitude observed in η electroproduction. Numerical comparison of the results has been carried out from the π and η photoand electroproduction data using the branching ratios, $\beta_{\pi N}$, $\beta_{\eta N}$, and $\beta_{\pi\pi N}$ channels from the fit at $0 \leq Q^2 \leq 4.5$ GeV^2. It was found ratios, $\beta_{\eta N} = 0.460 \pm 0.08 \pm 0.022$ and $\beta_{\pi N} = 0.485 \pm 0.008 \pm 0.023$. The single pion channel allows to extract the longitudinal component of helicity amplitude ($S_{1/2}$) due to the coupling between virtual photon and pion.

For the high resonance region ($W < 1.6$ GeV), in the absence of a coupled-multi-channel analysis framework for electroproduction channels, we subjected the differential cross section data to single channel energy-dependent partial wave analyses to extract the helicity amplitudes $A_{1/2}$, $A_{3/2}$, $S_{1/2}$ and their Q^2 dependence for some of the well-known isospin $\frac{1}{2}$ N^* states. Much of model sensitivity fit is due to the uncertainty in the non-resonant background amplitudes. Again, in order to have a quantitative measure of the sensitivity to the specific modeling of the background amplitudes in the fit we employed two independent approaches which are the unitary isobar model and the fixed-t dispersion relations.

The data [20; 37] cover the mass range up to 2 GeV, and are thus sensitive to many N^* and Δ^* states. All of these states were used in the global analysis. However, the single channel analysis does not allow the separation of the different isospin contributions. We have therefore limited our analysis to the determination of those resonances that are most sensitively probed in the $ep \to e'\pi^+ n$ channel, i.e. N^* states, and do not overlap with Δ^* states of the same spin and parity. We also restricted the analysis to masses below $W = 1.8$ GeV. This leaves the three states for which we show the resulting electrocoupling amplitudes, $N(1675)\frac{5}{2}^-$, $N(1680)\frac{5}{2}^+$, and $N(1710)\frac{1}{2}^+$.

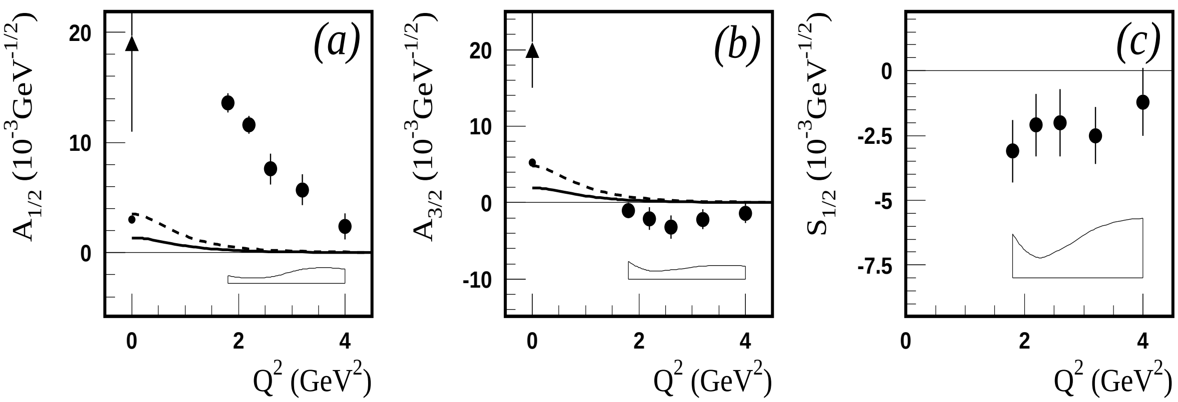

Fig. 3 Helicity amplitudes for the $\gamma^* p \to N(1675)\frac{5}{2}^-$ transition. The full circles are the results obtained in [37]. The bands show the model uncertainties. The dots at $Q^2 = 0$ are the predictions of the light-front relativistic quark model from Ref. [40]. The triangles at $Q^2 = 0$ are the RPP 2014 estimates [26]. The dashed and solid curves correspond to quark model predictions of Refs. [41] and [42], respectively.

Figure 3 shows the most intriguing results of our analysis for high lying resonance region. A large $A_{1/2}$ amplitude of the transition to the $N(1675)\frac{5}{2}^-$ state has been observed at all measured Q^2. This result is in contrast to several calculations of dynamical quark models that predict an order of magnitude smaller values than what is extracted from the data due to the Moorehouse selection rule. To our knowledge this is to date the strongest and most direct evidence for dominant non-quark contribution to the electroexcitation of a nucleon resonance on the proton. The situation with quark and meson-baryon contributions will become much clearer when data on neutrons become available.

For the beyond nucleon resonance region, we also have measured the cross sections ($d\sigma/dt$) of exclusive electroproduction of π^+ mesons from protons as a function of t = 0.1 - 5.3 GeV^2, x_B = 0.16 - 0.58, and Q^2 = 1.6 - 4.5 GeV^2 [43]. We have compared our differential cross sections to four recent calculations [44; 45; 46; 47] based on hadronic and partonic degrees of freedom. The four models give a qualitative description of the overall strength and of the t-, Q^2- and x_B- dependencies of our unseparated cross sections. There is an obvious need for $L - T$ separated cross sections in order to distinguish between the several approaches. These separations will be possible with the upcoming JLab 12-GeV upgrade. In particular, if the handbag approach can accommodate the data, the $p(e, e'\pi^+)n$ process offers the outstanding potential to access transversity GPDs. We have also several final states data ($K^+\Lambda$, $K^+\Sigma$, $\pi^0 p$) from resonance region to this deep inelastic kinematic regime to be analyzed together in a coupled channel framework [38; 39].

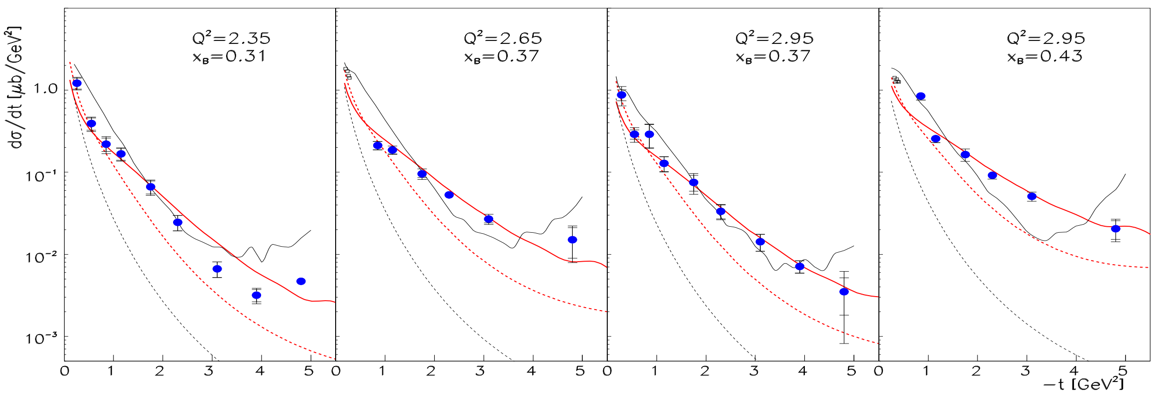

Fig. 4 (color online). Differential cross sections $d\sigma/dt$ [$\mu b/\mathrm{GeV}^2$] integrated over ϕ^*_π for various (Q^2, x_B) bins. The blue solid points are the present work. The error bars (outer error) on all cross sections include both statistical (inner error) and systematic uncertainties added in quadrature. The black open squares ($d\sigma/dt$) [48] and open stars ($d\sigma_L/dt$) [49] are JLab Hall C data. The red thick solid ($d\sigma/dt$), and dashed ($d\sigma_L/dt$) curves are the calculations from the Laget model [45] with (Q^2, t)-dependent form factors at the photon-meson vertex. The black thin solid ($d\sigma/dt$) and dashed ($d\sigma_L/dt$) curves are the calculations from the Kaskulov *et al.* model [46].

The selective single pion exclusive data set presented in this proceeding, for the first time has been explored full scale of W range from the threshold to DIS (< 2.4 GeV) and wide range of $Q^2 = 1.8-4.0$ GeV^2 and nearly 4π solid CM angle. This will allow to determine the transition charge and current densities of individual states through a Fourier transformation of the transverse amplitudes in the light cone frame. Such data can reveal novel information of the internal structure of the excited states in transverse impact parameter space [50].

References

1. R. G. Edwards, J. J. Dudek, D. G. Richards and S. J. Wallace, Phys. Rev. D **84**, 074508 (2011).
2. I. G. Aznauryan and V. D. Burkert, Prog. Part. Nucl. Phys. **67**, 1 (2012).
3. V.D. Burkert and T.-S. H. Lee, Int. J. Mod. Phys. E **13**, 1035 (2004).
4. K. Joo *et al.* [CLAS], Phys. Rev. Lett. **88**, 122001 (2002).
5. K. Joo *et al.* [CLAS], Phys. Rev. C**68**, 032201 (2003).
6. N. F. Sparveris *et al.*, Phys. Rev. C**67**, 058201 (2003).
7. A. Biselli *et al.* [CLAS], Phys. Rev. C**68**, 035201 (2003).
8. J. Kelly *et al.*, Phys. Rev. Lett. **95**, 102001 (2005).
9. S. Stave *et al.*, Eur. Phys. J. A**30**, 471-476 (2006).
10. M. Ungaro *et al.* [CLAS], Phys. Rev. Lett. **97**, 112003 (2006).
11. N. F. Sparveris *et al.*, [arXiv:nucl-ex/0611033].
12. D. H. Lu, A. W. Thomas, and A. G. Williams, Phys. Rev. C **55**, 3108 (1997).
13. A. Faessler, T. Gutsche, B.R. Holstein *et al.*, Phys. Rev. D **74**, 074010 (2006).
14. S. S. Kamalov and S. N. Yang, Phys. Rev. Lett. **83**, 4494 (1999).
15. S. S. Kamalov *et al.*, Phys. Rev. C **64**, (R) 032201 (2001).
16. T. Sato and T.-S. H. Lee, Phys. Rev. C **63**, 055201 (2001).
17. A. Matsuyama, T. Sato, and T.-S.H. Lee, Phys. Rep. **439**, 193 (2007).
18. B. Juliá-Díaz, T.-S.H. Lee, A. Matsuyama, and T. Sato, Phys. Rev. C **77**, 045205 (2008).
19. H. Egiyan *et al.* [CLAS], Phys. Rev. C **73**, 025204 (2006).
20. K. Park *et al.*, [CLAS], Phys. Rev. C **77**, 015208 (2008).
21. G. V. Fedotov *et al.* [CLAS], Phys. Rev. C **79**, 015204 (2009).
22. G. Ramalho and K. Tsushima, Phys. Rev. D **81**, 074020 (2010).
23. G. Ramalho and M. T. Pea, Phys. Rev. D **89**, 094016 (2014).
24. G. Ramalho and M. T. Pena, Phys. Rev. D **84**, 033007 (2011).
25. I. G. Aznauryan *et al.*, Int. J. Mod. Phys. E**22** 1330015 (2013).
26. K. A. Olive *et al.* [Particle Data Group Collaboration], Chin. Phys. C **38**, 090001 (2014).

27. K. Park *et al.*, [CLAS], Phys. Rev. C**85**, 035208 (2012).
28. V. M. Braun, D. Yu. Ivanov, A. Lenz and A. Peters, Phys. Rev. D **75**, 014021 (2007).
29. I. G. Aznauryan, Phys. Rev. C **67**, 015209 (2003).
30. I. G. Aznauryan, Phys. Rev. C **68**, 065204 (2003).
31. I. G. Aznauryan, V. D. Burkert, H. Egiyan, *et al.*, Phys. Rev. C **71**, 015201 (2005).
32. I. G. Aznauryan, V. D. Burkert, *et al.*, Phys. Rev. C **72**, 045201 (2005).
33. I. G. Aznauryan *et al.*, [CLAS], Phys. Rev. C **80**, 055203 (2009).
34. C. Armstrong *et al.*, Phys. Rev. D **60**, 052004 (1999).
35. R. Thompson *et al.* [CLAS], Phys. Rev. Lett. **86**, 1702, (2001).
36. H. Denizli *et al.* [CLAS], Phys. Rev. C **76**, 015204 (2007).
37. K. Park *et al.* [CLAS], Phys. Rev. C. **91**, 045203 (2015).
38. D. S. Carman, K. Park *et al.* [CLAS], Phys. Rev. C **87**, 025204 (2013).
39. M. Mestayer, K. Park *et al.* [CLAS], Phys. Rev. Lett. **113** 15, 152004 (2014).
40. I. G. Aznauryan and A. S. Bagdasaryan, Yad. Fiz. **41**, 249 (1985); translation in Sov. J. Nucl. Phys. **41**, 158 (1985).
41. D. Merten, U. Löring, B. Metsch, and H. Petry, Eur. Phys. J. A **18**, 193 (2003).
42. E. Santopinto and M. M. Giannini, Phys. Rev. C **86**, 065202 (2012).
43. K. Park *et al.* [CLAS], Eur. Phy. J. A **49**, 16(2013).
44. S. V. Goloskokov and P. Kroll, Eur. Phys. J. A **47**, 112 (2011).
45. J. M. Laget, Phys. Rev. D **70**, 054023 (2004).
46. M. M. Kaskulov, K. Gallmeister and U. Mosel, Phys. Rev. D **78**, 114022 (2008).
47. M. M. Kaskulov and U. Mosel, Phys. Rev. C **81**, 045202 (2010).
48. X. Qian *et al.*, Phys. Rev. C **81**, 055209 (2010).
49. T. Horn *et al.*, Phys. Rev. C **78**, 058201 (2008).
50. L. Tiator and M. Vanderhaeghen, Phys. Lett. B **672**, 344 (2009).